to yield significant amounts of IF(B-X) emission. In addition to the cooperative mechanism outlined above, this emission could also result from pumping by NCl(a) without participation of NF(a), in a manner analogous to the known pumping of IF(B) by O_2(a), or by the action of NF(b) independent of NCl(a), as previously recorded in this laboratory.[51,55] These prior (NF/IF transfer) experiments also demonstrated that NF(a) was not effective at producing the IF(B) state in the absence of other energetic species. In the present experiments, the IF(B-X) emission was reduced approximately 4-fold upon elimination of the FN_3. This result demonstrates that the majority of the observed IF(B-X) emission requires either NF(a) or NF(b). By adding trace I_2, to greatly enhance the NF(b) yield, at the expense of NF(a) and NCl(a), it was possible to show that only a very small fraction of the observed emission was due to transfer from the b state, since the yield of IF(B) was found to decline. Consequently, our data tends to support a cooperative mechanism involving both NF(a) and NCl(a) such as energy pooling through the $^3\Pi_2$ state as the dominant mechanism for IF(B) production under the conditions of our experiment. Since we have not observed this intermediate state directly, however, we cannot rule out other cooperative mechanisms that may be based, for example, on ground-state intermediates in a high state of vibrational excitation.

The intensity of the IF(B-X) emission was found to scale linearly with CF_3I addition up to 500 mTorr, which is well in excess of any potential for F-atom generation in our experiment. Therefore, it is unlikely that the IF(X) resulted from the fast reaction[56]

$$F + CF_3I \rightarrow CF_3 + IF \qquad (12)$$

because the yield of IF(B-X) emission would have saturated once the F atoms were titrated against the CF_3I. Since prior results tend to indicate a paucity of F atoms in our reactor, it appears that thermal or energy transfer induced disproportionation of CF_3I is a more likely source of ground-state IF. This mechanism, which does not require F atoms, would yield the observed linear dependence upon CF_3I addition. Disproportionation of the perfluoroiodide, however, is expected to be a very weak (low yield) source of the ground-state interhalogen, in which case the production of IF(B) may be throttled by IF(X) generation rather than the efficiency of pumping by NF(a) and NCl(a). Also if NF(a) is required to generate the IF(X) from CF_3I, then pumping to the B state can occur (consistent with our observations) solely due to the presence of NCl(a). Therefore, an effective thermal source of IF(X) will have to be developed and characterized before the mechanism and pump rates can be evaluated quantitatively.

(55) Pritt, A. T.; Patel, D.; Benard, D. J. *Chem. Phys. Lett.* **1983**, *97*, 471.
(56) Stern, L.; Wanner, J.; Walther, H. *J. Chem. Phys.* **1980**, *72*, 1128.

Summary

Reaction of Cl_2 with moist NaN_3 efficiently generates ClN_3, which has a barrier to dissociation of approximately 0.8 eV and a near gas kinetic rate of thermal excitation by collisions with the buffer gas. Thermal dissociation of ClN_3 occurs on the 1-10 μs time scale in ~100 Torr of Ar gas buffer at temperatures near 1200 K. The products are primarily NCl(a) and N_2, with a small fraction (<1%) as NCl(b). The radiative lifetime of NCl(a) is thought to be approximately 1.4 s and self-annihilation of NCl(a) may limit the kinetic lifetime of this species at high concentration. By use of a pulsed CO_2 laser and SF_6 as a sensitizer, transient concentrations of NCl(a) as large as 3×10^{15}/cm^3 have been obtained. The NCl(a) molecules are capable of generating I* by resonant energy transfer (similar to the O_2-I interaction) and the I* may be used to upconvert NF(a) to NF(b). Cooperative pumping of IF(B) by NCl(a) and NF(a) appears to be limited by the availability of IF(X) due to a lack of F atoms and does not involve NF(b) as a precursor, but may be the result of an energy pooling mechanism that proceeds through the IF($^3\Pi_2$) state as an intermediate. Further studies are required to determine the potential of these and similar mechanisms for the generation of visible laser radiation from the electronic energy that is stored in the singlet metastable products of thermally dissociated halogen azides.

Acknowledgment. The electronic structure calculations were supported in part by the Air Force Astronautics Laboratory under contract No. F04611-86-C-0071.

Photofragmentation Pathways of a PMMA Model Compound under UV Excimer Laser Ablation Conditions

S. Küper, S. Modaressi, and M. Stuke*

Department Laserphysik, Max-Planck-Institut für biophysikalische Chemie, P.O. 2841, D-3400 Göttingen, Federal Republic of Germany *(Received: January 30, 1990)*

A model compound for the polymer poly(methyl methacrylate) (PMMA) was synthesized and investigated under UV excimer laser photolysis of different wavelengths and pulse durations in hexane solution. Qualitative analysis of the photolysis products reveals a well-defined photochemical fragmentation pattern of the PMMA model system. Quantitative analysis shows that the major primary process in the photolysis of this type of molecules is the side-chain scission under formation of double bonds. Depending on the irradiation conditions, a quantum yield of $\Phi = 0.5 \pm 0.1$ is observed for 248-nm, 16-ns laser radiation. The high quantum yield and the strong analogy of the model system to the behavior of PMMA under 248-nm ablation show that the photochemical contribution to the ablation process at this wavelength is far from negligible.

Introduction

The ability of controlled material removal by UV excimer laser ablation[1,2] has raised considerable interest due to its proven and potential applications in electronic manufacturing and surgery. A variety of materials ranging from polymers to biological tissue was successfully structured or cut by ablation showing little or no damage to the remaining material, and the achievable spatial resolution of excimer laser induced microstructures has been shown to be well below 1 μm.[3] While ablation has already found numerous applications in industry[4] and surgery,[5] a detailed un-

(1) Kawamura, Y.; Toyoda, K.; Namba, S. *Appl. Phys. Lett.* **1982**, *40*, 374; *J. Appl. Phys.* **1982**, *53*, 6489.
(2) Srinivasan, R.; Mayne-Banton, V. *Appl. Phys. Lett.* **1982**, *41*, 576.
(3) Rothschild, M.; Ehrlich, D. J. *J. Vac. Sci. Technol. B* **1987**, *5*, 389.

0022-3654/90/2094-7514$02.50/0

derstanding of the ablation process, particularly its chemistry, still remains a challenge.

It is widely accepted that both photochemical and thermal processes can produce the necessary increase in the specific volume, which causes the explosive ejection of material. For many polymers, however, the question of the dominating contribution is still a matter of controversy. A key to understanding the mechanism of ablation is a precise analysis of the material before, during, and after ablation. Therefore, great attention has been paid to the fragments leaving the surface of polymers under ablation, and particles ranging from diatomics to molecules several times larger than the monomer have been detected by laser-induced fluorescence,[6,7] time of flight mass spectroscopy,[8,9] and emission spectroscopy.[10]

For a good understanding of the chemistry of ablation it is highly desirable to determine the exact fragmentation pattern, i.e., the actual sites of bond scission following the excitation of the polymer with UV light, and the quantum yield of the photolysis. A natural property of polymers is that they do not consist of a single type of molecules but have a broad molecular mass distribution. Due to this fact and to their high molecular weight, any kind of photolytic or thermal degradation produces a mixture of an almost unlimited number of different compounds with formula weights ranging from some ten to several thousand atomic mass units. Because of this lack of defined fragments the determination of exact bond scission sites or a complete fragmentation pattern of most polymers is a difficult problem. In the case of poly(methyl methacrylate) (PMMA) it has been shown qualitatively that the fission of methyl formate from the polymer chain[9,11] under production of unsaturated units[12] in the polymer chain is a major photochemical process following irradiation with pulsed or continuous UV light of wavelengths below 270 nm.

Electron spin resonance (ESR) spectroscopy and NMR of PMMA samples, irradiated under various conditions, provide information about the primary radical photoproducts.[12,13] However, the complete assignment of the spectrum is still under discussion. Furthermore, the question of the radicals' subsequent reactions, and therefore the actual photoproducts, cannot be solved by this method.

A different approach to this problem is the *synthesis of model compounds*, which represent a piece of the polymer chain containing a small number of monomer units. The photolysis of these model compounds yields a number of primary radical photofragments, which in the chemical environment of a hexane solution stabilize either by tearing off a hydrogen atom from a solvent molecule or by elimination of another small radical, thus forming unsaturated species. The resulting stable photoproducts typically have molecular weights that allow a convenient separation by gas chromatography. By subsequent spectroscopic analysis (infrared, ultraviolet, nuclear magnetic resonance, and mass spectroscopy) the compounds can be identified unambiguously. Often the possible photoproducts are commercially available and can thus serve for a convenient comparison of retention times and spectra. A complete qualitative analysis of the stable photoproducts reveals the sites of primary bond scission following electronic excitation and their subsequent reactions. Additional quantitative analysis of the irradiated mixtures further allows the determination of the relative probabilities for a scission at different sites of the molecule and the quantum yield of the photolysis.

In this paper we shall describe the detailed study of a PMMA model compound and its photolysis with excimer laser light of different wavelengths and intensities. As a model for PMMA, 2,2,4,4-tetramethylglutaric acid, dimethyl ester (**1**) was chosen, which represents a piece of the polymer chain containing two monomer units with its two chromophores (see Figure 1). In order to better simulate the main polymer chain, higher substituted compounds like 2,4-diethyl-2,4-dimethylglutaric acid, dimethyl ester (**2**), were also synthesized; however, they complicate the analysis due to the existence of several steric isomers. More importantly, the presence of hydrogen atoms in γ-position to the carboxyl group would allow Norrish type II fragmentations, which are not possible in PMMA. Therefore, higher substituted molecules like **2** are unsuitable for a simulation of PMMA.

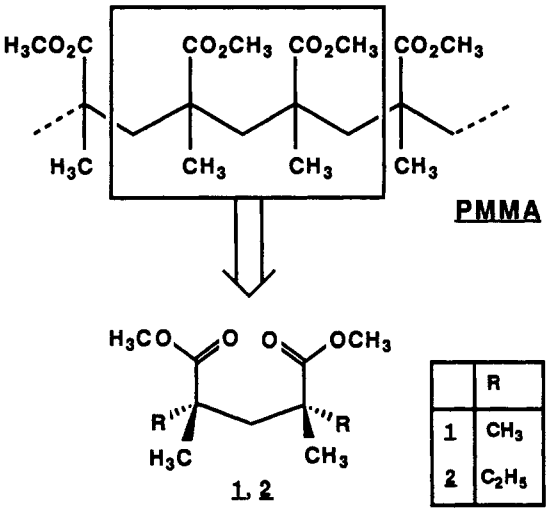

Figure 1. Structure of poly(methyl methacrylate) (PMMA) showing the origin of the model compound 2,2,4,4-tetramethylglutaric acid, dimethyl ester (**1**), as a part of the polymer chain.

Experimental Section

Compounds. **1** was synthesized starting from 2,4-dimethylglutaric acid, which was first converted to the dimethyl ester by standard synthesis methods. The product was deprotonated with 2.15 equiv of lithium diisopropylamide (LDA) in tetrahydrofuran at −77 °C in the presence of HMPT followed by alkylation with 2.15 equiv of methyl iodide. The resulting **1** (colorless crystals, mp 30 °C) was purified by repeated sublimation in vacuo. The UV spectra of **1** and PMMA are qualitatively identical. Both show a weak absorption band at 214 nm and are virtually transparent for light of wavelengths longer than 260 nm. The molar extinction coefficient ϵ of **1** is 75.6 at 193 nm, 224.1 at 214 nm, 3.6 at 248 nm, and <0.5 L/(mol·cm) at 308 nm.

Methanol (**3**), methyl formate (**4**), methyl isobutyrate (**5**), methyl methacrylate (**6**), and methyl pivalate (**7**) are commercially available (Aldrich) and were used without further purification.

Light Sources. Sources of nanosecond UV laser radiation were Lambda Physik EMG 501, EMG 200, and EMG 103 MSC excimer lasers with the appropriate filling of halogen and noble gases for operation at 193, 248, and 308 nm, respectively. In order to exclude possible effects due to heating of the solvent, the repetition rate of the laser was kept below 5 Hz.

Subpicosecond excimer laser pulses at 248 nm were obtained from a system by Szatmári and Schäfer[14] using a Lambda Physik EMG-150 dual channel excimer laser and an EMG 401 large-aperture amplifier. The system delivers 500-fs pulses of 60-mJ energy with a fraction of less than 1% amplified spontaneous emission (ASE). For all laser sources the pulse energy was measured with a pyroelectric energy meter. Energy measurements were averaged over ten pulses and are within an uncertainty of ±10%.

Procedure. **1** was dissolved in hexane with a known concentration of ~0.2 mol/L. The solutions were irradiated in Suprasil

(4) Bachmann, F. *Chemtronics* **1989**, *4*, 149 and references therein.
(5) Birngruber, R. *Dev. Opthal.* **1987**, *14*, 47–68.
(6) Srinivasan, R.; Braren, B.; Dreyfus, R. W. *J. Appl. Phys.* **1986**, *61*, 372.
(7) Srinivasan, R.; Braren, B.; Dreyfus, R. W.; Hadel, L. *J. Opt. Soc. Am. B* **1986**, *3*, 785.
(8) Larciprete, R.; Stuke, M. *Appl. Phys. B* **1987**, *42*, 181.
(9) Estler, R. C.; Nogar, N. S. *Appl. Phys. Lett.* **1989**, *49*, 1175.
(10) Koren, G.; Yeh, J. T. C. *J. Appl. Phys.* **1984**, *56*, 2120.
(11) Gupta, A.; Liang, R.; Tsay, F. D.; Moacanin, J. *Macromolecules* **1980**, *13*, 1696.
(12) Küper, S.; Stuke, M. *Appl. Phys. A* **1989**, *49*, 211.
(13) Torikai, A.; Fueki, K. *J. Photochem. Photobiol. A* **1989**, *49*, 273.
(14) Szatmári, S.; Schäfer, F. P. *Opt. Commun.* **1988**, *68*, 196.

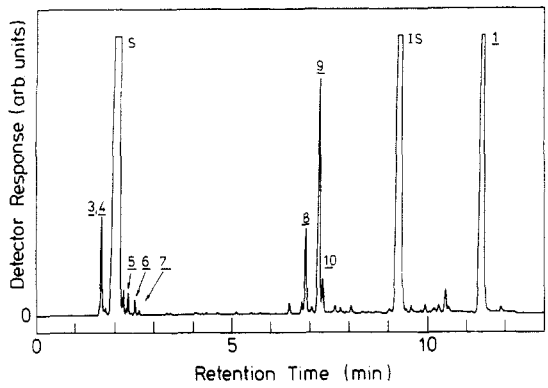

Figure 2. Gas chromatogram of a hexane solution of (**1**) after irradiation with 3000 pulses of 480 mJ/cm² at 248 nm. The chromatogram displays a number of defined peaks, most of which can be assigned unambiguously to specific compounds. Peaks are labeled with the reference number of the assigned compound (compare Figure 3). IS = internal standard (undecane), S = solvent (hexane).

quartz cells with an optical path length of 1 mm. To prevent the evaporation of volatile photolysis products, all cells were sealed with rubber septa and irradiated solutions were transferred for subsequent analysis via canula.

Qualitative analysis of the product mixtures was carried out on a Hewlett Packard 5992B gas chromatograph/mass spectrometer (GC/MS) equipped with a Hewlett Packard OV-101 quartz capillary column of 50 m length using helium as carrier gas. Fragments, which could not be identified unambiguously by comparison of their mass spectra and retention times with those of commercially available compounds, were isolated by preparative gas chromatography on packed columns in sufficient quantity for identification by infrared and nuclear magnetic resonance (NMR) spectroscopy.

Quantitative analysis of the product mixtures was carried out on an Intersmat IGC 131 programmable gas chromatograph equipped with flame ionization detector (FID) and Hewlett Packard 3390 A integrator. The free induction decay (fid) was calibrated with mixtures of the fragments with known concentrations for compounds **1** and **3–7**, which are readily available. Undecane was used as internal standard; its use was limited to the laser wavelengths of 248 and 308 nm, however, since it is not inert toward 193-nm laser irradiation. The response factors of fragments, which were not available in sufficient quantity, were extrapolated from the data of similar compounds, making use of the fact that within one class of compounds (e.g., aliphatic mono esters) the detector response per mole shows good linearity to the molecular mass of the compound. To exclude the influence of secondary reactions on the composition of the irradiated solutions, they were analyzed after different irradiation doses (i.e., different degrees of conversion). Quantitative GC measurements are accurate within an uncertainty of ±10%. Quantum yields Φ were calculated by comparing the decrease in the concentration of **1** with the absorbed photon dose and are accurate within an error of ±20%.

Results

Solutions of **1** in *n*-hexane are readily photolyzed by UV laser light of 193 and 248 nm, while 308-nm laser radiation leaves the compound unaffected within experimental uncertainty, even after exposure to 50 000 pulses of 42 mJ/cm².

In the case of 193- and 248-nm wavelength, a decay in the concentration of **1** after excimer laser irradiation is observed in the gas chromatogram, while a number of new, well-defined peaks appear. Their intensity rises with a growing irradiation dose. A typical gas chromatogram of a solution of **1** in hexane after irradiation with 3000 pulses of 480 mJ/cm² at 248 nm is shown in Figure 2. Qualitative analysis of the irradiated solutions allows the assignment of all major peaks in the chromatogram to the compounds **3–10**, and reveals the complete fragmentation pattern of **1** under UV photolysis (see Figure 3). Compounds **3**, **4**, and **8–10** are the fragments of a side-chain scission, while the species **5–7** are the products of a main-chain scission of the model compound. **3–7** were not produced in a quantity sufficient for a complete spectroscopic investigation but are readily identified by matching retention times *and* mass spectra with those of purchased samples. Methanol (**3**) and methyl formate (**4**) have identical retention times under the chromatographic conditions applied for Figure 2, but are separated at lower temperatures for quantitative analysis. Compounds **8**, **9**, and **10**, which are the major photoproducts, were isolated by preparative gas chromatography and unambiguously identified by a complete set of IR, NMR, and mass spectra.

The number of fragments and the molecular structure of the photolysis products is insensitive to a change in the laser wavelength from 193 to 248 nm and a variation of the average light intensity from 0.094 to 22 000 MW/cm²; the relative abundance

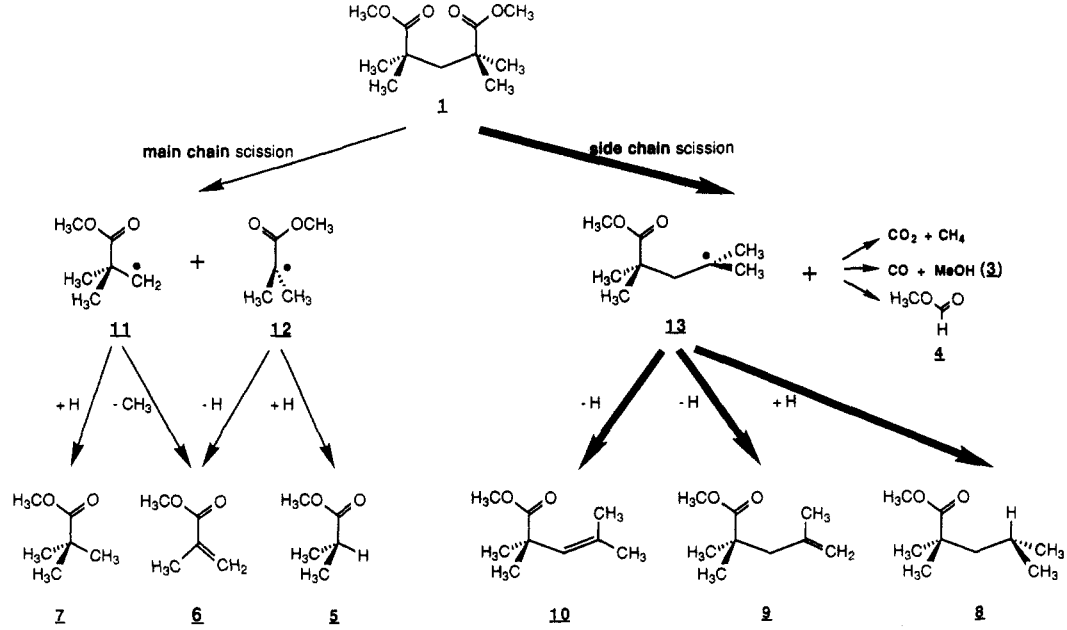

Figure 3. Fragmentation scheme of the PMMA model system **1**. Both side- and main-chain scission are observed after photolysis with UV excimer laser light of 248-and 193-nm wavelength; the side-chain scission is by far the dominating process, however. The resulting methoxycarbonyl and chain radicals **13** stabilize preferably by formation of methyl formate, the unsaturated compounds **9** and **10**, and the saturated product **8**. The relative yields of the fragments with respect to the decrease of **1** are given in Table I for different irradiation conditions.

TABLE I

wavelength, nm	fluence, mJ/cm²	mean intensity, MW/cm²	rel amounts (%) = 100[i]/([1]₀ − [1]ₙ)								quantum yield Φ
			3	4	5	6	7	8	9	10	
193	36	1.0			<0.1	1.9	<0.1	8.6	12.4	0.5	
248	3.3	0.094	10.1	18.0	<0.1	<0.1	<0.1	15.6	34.6	2.9	0.58
248	45	1.28	20.7	31.9	1.3	1.3	<0.1	16.6	48.3	4.3	0.53
248	480	13.7			4.1	4.5	0.3	8.6	35.8	5.0	0.42
248	11	22000			1.3	1.64	0.7	17.6	43.3	3.6	
308	42	1.2	<0.1	<0.1	<0.1	<0.1	<0.1	<0.1	<0.1	<0.1	>0

of the fragments, however, is affected by the irradiation conditions.

The quantitative gas chromatographic analysis of the irradiated solutions provides the absolute amounts of all observed fragments of **1**. The relative amounts with respect to the decrease in the concentration of **1**, which reveal the abundance of the different photolytic reaction paths, are calculated by

$$\text{relative amount } (i) = 100[i]/([\mathbf{1}]_0 - [\mathbf{1}]_n) \qquad (1)$$

where $[i]$ is the concentration of fragment i, $[\mathbf{1}]_n$ is the concentration of **1** after n laser pulses and $[\mathbf{1}]_0$ before irradiation. For small degrees of conversion (<30%) the relative amounts of the photoproducts are insensitive to the irradiation dose (i.e., number of pulses). Under photolysis conditions directly affecting hydrocarbons (i.e., <200-nm wavelength or very high light intensities) methanol (**3**) and methyl formate (**4**) are not resolvable in the chromatogram, because their peaks are covered by those of solvent fragments. The complete results of the quantitative analysis after photolysis under various conditions are given in Table I.

Depending on the irradiation conditions the quantitative analysis registers between 49 and 72% of the photolyzed **1** in the form of the fragments shown in Figure 3. Under all photolytic conditions compounds **8**, **9**, and **10**, which are the products of a side-chain scission, dominate the fragmentation pattern with a relative abundance between 49 and 69%, whereas the *fragments from a main-chain scission*, **5**, **6**, and **7**, *never reach an abundance exceeding 4.5%*. No drastic changes in the composition of the photolysis mixtures are observed even though the laser light intensity was varied by more than 6 orders of magnitude. The relative abundance of a main-chain scission, however, rises by a factor of 40 with the fluence being increased by 2 orders of magnitude in the range of 5–500 mJ/cm².

The total quantum yield Φ of the photolysis of **1** is calculated by comparing the absolute amount of photolyzed **1** ($[\mathbf{1}]_0 - [\mathbf{1}]_n$) with the number of absorbed quanta after various irradiation doses. The number of absorbed quanta was calculated by using the measured low-intensity transmission of the sample solutions. Since hexane loses its transparency at high light intensities and wavelengths below 200 nm, useful quantum yields can only be obtained with this method at wavelengths >200 nm and low intensities. Since, furthermore, the assumption of a constant absorption is only true for low irradiation doses,[12] the photolysis was carried out only to small degrees of conversion for quantum yield measurements.

The obtained quantum yield for 248 nm is 0.58 at 3.3 mJ/cm² and 0.53 at 45 mJ/cm², while at much higher fluences solvent effects come in. The yield is constant within experimental uncertainty for a variation of the average light intensity by 1 order of magnitude and changes little after an increase by a factor of more than 100. In the latter case, however, the chromatogram already shows peaks of solvent degradation, a sign that its absorption is no longer negligible. In the case of 193-nm wavelength or femtosecond excimer laser irradiation the pure solvent's absorption either is or becomes after a few laser pulses larger than the absorption of the model compound **1** itself, a fact which does not allow useful quantum yield calculations.

Discussion

The degradation of the model compound **1** with laser light of moderate fluences in a hexane solution is without doubt a photochemical process. A thermal degradation of the sample can be excluded, since hexane has a boiling point of only 69 °C, a temperature far too low for a pyrolysis of **1**.

Almost all possible fragments of **1** are found in the analysis of the photolyzed mixture. The high relative abundance of **8**, **9**, and **10** shows that the most probable process following electronic excitation of the carboxyl group is its fission from the main carbon chain, either as a whole methoxycarbonyl radical or in form of its fragments methyl radical and carbon dioxide or methoxy radical and carbon monoxide. The detection of methanol and methyl formate proves the existence of two of the mentioned reaction channels, and the third one can by no means be excluded since methane and CO_2 were not analyzed with our present GC/MS setup. In the relatively unreactive environment of a hydrocarbon solution, the resulting chain radical **13** stabilizes either by eliminating a hydrogen atom leading to the unsaturated isomeric photofragments **9** or **10**, which is the preferred reaction, or by tearing off a hydrogen atom from a solvent molecule, thus forming **8**. *The main-chain scission* leading to the radicals **11** and **12** *is only a minor process*. It is not surprising that the transport of sufficient energy to break a bond along the carbon chain without relaxation into the various degrees of freedom is highly unlikely. Nevertheless, the compounds **5**–**7**, which are the stabilization products of the radicals **11** and **12** are clearly detected after their formation due to *main-chain scission* and their relative yields *rise with an increasing fluence* (not intensity). Since the main-chain scission is the sole degradation process upon heating of PMMA, this indicates the existence of highly vibrationally excited molecules and thus can be considered as the photothermal contribution to the degradation of **1**. In the latter case the weakest bond is broken leading to **11** and the stabilized heteroallyl radical **12**.[15]

The measured quantum yield Φ of 0.5 ± 0.1 is quite high for a photolysis in the condensed phase but is in fair agreement with the values observed by others.[11] It proves that the dissociation of the carboxyl group from either a repulsive electronic state or a highly vibrationally excited state successfully competes with the relaxation of the photonic energy into heat. The fact that Φ is almost constant for a variation of the laser intensity by a factor of 100 shows that the photolysis of **1** by nanosecond excimer laser radiation is a one-photon process. The effect of femtosecond excimer laser irradiation, where coherent two-photon absorption has to be taken into account, on the photolysis of **1** cannot be precisely measured with this method, because of the strong absorption of any solvent at intensities on the order of GW/cm². Since the fragmentation pattern is the same both for nanosecond and femtosecond laser irradiation, it has to be assumed that a coherent two-photon excitation of **1** in hexane does not result in different photoproducts, but merely a higher quantum yield for dissociation.

The model compound **1** shows excellent analogy to PMMA in its properties and its behavior under UV irradiation. Both compounds have an absorption maximum at 214 nm, which can be assigned to the $n \rightarrow \pi^*$ transition of the carboxyl group. The absorption cross section for one chromophore at 248 nm is 1.44×10^{-20} cm² for PMMA and 0.68×10^{-20} cm² for **1**. The volatile photoproducts of **1** like methyl formate, carbon monoxide, and methanol are observed both in the incubation and ablation of PMMA and the photolysis of **1**. PMMA and **1** display an increasing UV absorption upon UV irradiation, which can be explained with the production of unsaturated species. These analogies show that **1** is an excellent model compound to study

(15) Birkhofer, H.; Beckhaus, H.-D.; Rüchard, C. In *Substituent Effects in Radical Chemistry*; Viehe, H. G., Janousek, Z., Merényi, R., Eds.; NATO ASI Series C; Kluwer: Dordrecht, 1986; Vol. 189, p 199.

the behavior of the polymer PMMA.

Conclusion

Under the legitimate assumption that PMMA and **1** behave similarly also with respect to phenomena, which cannot be measured directly, a number of conclusions for the photochemistry and ablation of PMMA can be drawn from this study: (1) PMMA type compounds undergo photolysis with a high quantum yield for wavelengths of 248 nm or shorter. (2) The quantum yield Φ for the photolysis at 248 nm is $\Phi = 0.5 \pm 0.1$. (3) The photolysis is a one-photon process. (4) The main photoreaction is the side-chain scission of the carboxyl group either as methyl formate or in form of smaller fragments like carbon monoxide and methanol or carbon dioxide and methane. The remaining chain radical preferably stabilizes by elimination to form unsaturated species. (5) The main-chain scission is observed but is only a minor photolytic process. (6) Taking the high quantum yield for the photolysis of the ester carboxyl group to several gaseous or volatile fragments into account, it can be concluded that the photochemical contribution to the ablation of PMMA at wavelengths $\lambda \leq 248$ nm is far from negligible.

Acknowledgment. We thank K. Müller and W. Sauermann for their technical assistance and S. Szatmári and F. P. Schäfer for the opportunity to use their source of femtosecond excimer laser radiation at 248 nm. Financial support by Bundesministerium für Forschung und Technologie (BMFT No. 13N5398/7) is gratefully acknowledged.

Registry No. 1, 34372-00-4; PMMA, 9011-14-7.

Photoexcitation and Photoluminescence Study of Coordination Complexes of Lead Diiodide with Pyridine

L. C. Yu-Hallada and A. H. Francis*

Department of Chemistry, The University of Michigan, Ann Arbor, Michigan 48109
(Received: February 5, 1990)

PbI_2 exhibits a lamellar CdI_2 crystal structure, similar to that of transition-metal dichalcogenides (MX_2) and transition-metal phosphorus trichalcogenides (MPX_3). When PbI_2 is exposed to any of a variety of organic Lewis bases, it undergoes a solid-state reaction that produces a material with a substantially altered electronic spectrum. Because the reaction is similar to the intercalation reactions of the lamellar chalcogenide lattices with Lewis bases, the reaction of PbI_2 has also been described as an intercalation reaction. Examination of the liquid helium temperature photoexcitation and photoluminescence spectra of the reaction product with pyridine suggests that there are important differences between the reaction products of the lamellar chalcogenide lattices and PbI_2 with organic Lewis bases. The latter may be described better as coordination compounds resulting from a heterogeneous reaction between solid PbI_2 and the vapor or liquid phase of the organic ligand.

I. Introduction

Lead diiodide is a layered compound whose crystals form hexagonal lattices with the CdI_2 structure. Each layer consists of nearly octahedrally coordinated divalent lead ions, sandwiched between sheets of iodide ions. The I–Pb–I unit is held together by strong (intralamellar) metal–halogen bonds. In contrast, the bonds between the neighboring molecular layers are weak van der Waals bonds. The structure is similar to that of the transition-metal dichalcogenide (MX_2) and phosphorus trichalcogenide (MPX_3) lattices. It is well-known that these transition-metal lattices undergo reversible, topotactic solid-state reactions with a variety of organic Lewis bases.[1] These reactions involve the intercalation of the interlamellar interstices or the van der Waals gap (VWG). In the process of intercalation, the host lattice may expand considerably along the stacking axis but the intralamellar bonding is not significantly altered. The reactions are frequently reversible under relatively mild conditions.

Reactions of PbI_2 with organic Lewis bases have been studied for many years. The reactions are generally carried out under conditions similar to those used for the intercalation of MX_2 or MPX_3 lattices and result in the uptake of considerable amounts of the Lewis base by the solid PbI_2 reactant. The products have generally been described as intercalation compounds, and there is extensive literature on the subject of their preparation and properties.

While there are structural similarities between the PbI_2 lattice and the MX_2 and MPX_3 lattices, the physical effects of reaction with Lewis bases are dramatically different. For example, large crystals of the chalcogenide lattices may be intercalated and remain intact. When PbI_2 crystals are reacted with Lewis bases, they rapidly disintegrate and form a finely dispersed powder with grain dimension < 1 μm. Whereas the transition-metal chalcogenide lattices undergo intercalation with significant changes in only the interlamellar spacing, PbI_2 adducts with Lewis bases generally exhibit large changes in the intralamellar dimensions as well.

Intercalation of the layered chalcogenide lattices with neutral Lewis bases produces relatively slight changes in the electronic spectrum of the host, usually amounting to less than a 0.1-eV shift in the band edge to lower energy.[2] In sharp contrast, when solid PbI_2 is exposed to pyridine, the absorption edge shifts to higher energy by approximately 0.8 eV. These observations and others suggest that there are substantial differences between the intercalation chemistry of the layered transition-metal chalcogenides and PbI_2. In the present work, we examine the low-temperature photoluminescence (PL) and photoexcitation (PE) spectra of compounds derived from treating PbI_2 with pyridine. We compare the PL and PE spectra with previously published absorption spectra of PbI_2 thin evaporated films and colloidal suspensions in order to better characterize the products of the solid-state reaction. The PE spectra are particularly useful in identifying the spectroscopic effects of impurities and observing spectral features near the fundamental absorption edge.

II. Experimental Section

Sample Preparation. Reagent-grade PbI_2 powder was obtained from the Aldrich Chemical Company and used without further

(1) See for example: Whittingham, M. S. In *Intercalation Chemistry*; Whittingham, M. S., Jacobson, A. J., Eds.; Academic Press: New York, 1982.

(2) Cleary, D. A.; Francis, A. H.; Lifshitz, E. *J. Luminesc.* **1986**, *35*, 163.

0022-3654/90/2094-7518$02.50/0